International Journal of Smart Grid and Clean Energy

Hybrid AC/DC transmission expansion planning based on coupling analysis with large integration of renewable energy

Hao Li, Ying Qiao, Zongxiang Lu

Department of Electrical Engineering, Tsinghua University, Beijing, 100084, China

Abstract

The promotion of renewable energy in distant areas faces problems with mismatch between generation and grid. Because the local demand is not enough to accommodate variable renewable energy, a proportion of renewable power need to be transmitted to external power systems via the local grid besides consumed by the local load, which poses a great challenge to the security control of the local grid. Such a relationship is called "coupling". To reduce the side effect of coupling in the stage of transmission planning, we firstly proposed coupling evaluation indicators in the perspective of the grid structure and system operation states and then presented a method to implement evaluation based on the economic dispatch model considering system's mitigation against fluctuations. Finally, a transmission expansion planning (TEP) method is proposed with the inclusion of coupling evaluation and the consideration of a hybrid AC/DC transmission system. The case study demonstrates the coupling and shows that hybrid AC/DC transmission is better when coping with such a situation than AC transmission system.

Keywords: Coupling, renewable energy, grid, transmission expansion planning, Hybrid AC/DC system

1. Introduction

In recent years, renewable energy has developed rapidly, and the deployment of renewable energy has become far from the load center, such as the Nordic wind power center [1] and the renewable energy center in Northwest China [2]. The demand near these centers is small and the affluent renewable energy power needs to be transmitted to external systems for efficient consumption. Considering the economy, a large amount of renewable energy needs to be sent out via the local grid. At the same time, peak-shaving power supply near the renewable energy base is insufficient, which needs additional regulation of conventional generators in the local power grid. In this situation, the fluctuated renewable energy would influence the local grid. For example, in 2011, faults in the Gansu and Hebei province of China caused wind turbines disconnection, with the loss of over 500MW [3].

The above problem is due to the fact that the renewable energy transmission grid partially overlaps with the local grid, leading to the conflict between renewable power transmission and security control in local grid. This relationship is called "coupling", which would cause operation states closer to the security boundary, such as congestion incidents and extreme voltage incidents. In order to stabilize the state fluctuation, the system needs to sacrifice part of the operational economy.

There are many researches concerning the impact of renewable energy on the operation status of power systems [4-6]. Reference [4] quantified the risk associated with wind power intermittency in California. Reference [5] analyzed three major challenges of integrating variable generation from wind and solar into power systems. Reference [6] investigated peak regulation of wind power integrated power systems. However, most of studies focused on the impact analysis of renewable energy on the system. Few of them combined impact analysis with system planning.

* Manuscript received November 25, 2020; revised June 9, 2021.
Corresponding author. *E-mail address*: h-l16@mails.tsinghua.edu.cn.
doi: 10.12720/sgce.10.3.215-223

DC transmission, which can regulate the power flow with less effort than AC transmission, has advantages in dealing with the volatility of renewable energy compared to AC transmission. Thus DC transmission is adopted in transmission system planning. At present, most of the planning scenarios for DC are long-distance and large-capacity transmission. With the rapid development of VSC-HVDC transmission technology, the coordinated cooperation of VSC-HVDC and AC grid will significantly increase the flexibility in grid operation. In the study of AC/DC hybrid transmission planning, Reference [7] proposed that the economic equivalent transmission distance cannot be used as the only criterion for determining DC lines in planning; [8~10] considered DC transmission to reduce power loss. Reference [11] considered the use of DC transmission to connect distant wind farms or photovoltaic power plants, [12] proposed the use of DC grid in the integration of distributed generation. In the above researches, [7~10] did not consider renewable energy and [11~12] did not pay enough attention to the volatility of renewable energy. Moreover, the above studies did not consider the effect of HVDC on the flexibility in local grids with high proportion of renewable energy.

This study focuses on the coupling problem of renewable energy output and system state in a system with high proportion of renewable energy. The distinction of renewable power transmission grid and local power supply grid is proposed based on power flow tracking method. The coupling evaluation indicators and method are established from the perspective of grid structure and operation state. In addition, a hybrid AC/DC transmission expansion planning method for power systems considering reducing coupling is proposed. The examples verify the proposed indicators and methods.

2. Coupling of Renewable Energy and Local Grids

2.1. Concept of coupling

In power grids integrated with large amount of renewable energy, part of the renewable power provides local load, while the remaining power is supposed to be transmitted to external systems for efficient consumption. Therefore, the grid has two functions: local power supply (denoted as Fun1), and external power transmission (denoted as Fun2). Due to the limitation of environment and policy, the construction of transmission lines directly to external systems lags behind the construction of the local grid. Thus, part of the renewable energy needs to be sent out through local grid. In addition, the flexibility resources near the renewable generation stations are far from enough. Thus, to ensure the steady power on external power transmission, local system needs to interact and coordinate with renewable energy.

From aspect of grid structure, the mentioned problems above are mainly due to the partial overlap between local grid and external power transmission grid, leading to the interaction and mutual influence between the fluctuated renewable energy and the operation status in local grid. The fluctuated renewable energy output would make system states closer to the security boundary. To cope with it, part of the renewable energy has to be curtailed when necessary. This kind of mutual influence and restriction is referred to as "coupling", leading to significant fluctuation in the system, which would result in an increase in the probability that the power flow and voltage approach the limit. The system operation would become much more complicated and part of the operational economy has to be sacrificed.

2.2. Distinction of grid functions

The functions of the grid are mainly distinguished by the purpose of power transmission. If the power transmitted on the line is for local load supply, then the line belongs to Fun1, and vice versa, the line belongs to Fun2. This paper implements the identification of functions based on the power flow tracking method [13]. Based on the principle of proportional distribution, the power flow tracing method determines the usage degree of each load node on the grid by tracking the active power flow.

Suppose that the set of nodes connected with local load is $\Omega_{\text{Node}}^{\text{local}}$ and the set of nodes connected with external system is $\Omega_{\text{Node}}^{\text{out}}$, then at time *t*, the lines belong to *Fun1* and *Fun2* can be grouped in different sets:

$$Line_{ij,t} \in \Omega_{\text{Line},t}^{\text{local}},\ \ if\ \ \left|P_{ij,t}^{Lk}\right| \neq 0,\ Node_k \in \Omega_{\text{Node}}^{\text{local}} \tag{1}$$

$$Line_{ij,t} \in \Omega_{\text{Line},t}^{\text{out}},\ \ if\ \ \left|P_{ij,t}^{Lk}\right| \neq 0,\ Node_k \in \Omega_{\text{Node}}^{\text{out}} \tag{2}$$

Due to the volatility of renewable energy, the functions of the lines varies at different time. In time period *T*, *Fun1* and *Fun2* are the union of the functions at each time, respectively.

$$\Omega_{Line,T}^{local} = \bigcup_{t \in T} \Omega_{Line,t}^{local} \tag{3}$$

$$\Omega_{Line,T}^{out} = \bigcup_{t \in T} \Omega_{Line,t}^{out} \tag{4}$$

3. Evaluation Indicators and Methods of Coupling

Based on the differentiation of grid functions in the previous section, considering the performance of the system in terms of power flow and voltage, this section evaluates the coupling from two aspects, coupling range and coupling depth.

3.1. Evaluation Indicators

- Range of Coupling (RoC)

  This indicator evaluates the proportion of the nodes which simultaneously belongs to both functions:

$$RoC = n(\Omega_{\text{Node}}^{\text{C}}) / n(\Omega_{\text{Node}}) \tag{5}$$

$$Node_i \in \Omega_{\text{Node}}^{\text{C}},\ if\ \ Line_{ij} \in \left(\Omega_{\text{Line,T}}^{\text{local}} \bigcap \Omega_{\text{Line,T}}^{\text{out}}\right) \tag{6}$$

where $n(\ )$ represents the number of elements in the set, $\Omega_{\text{Node}}^{\text{C}}$ represents the set of nodes which simultaneously belongs to both functions. The larger the ratio is, the wider the coupling range is.

- Depth of Coupling (DoC)

  The depth of coupling is evaluated by the distance between system state and security boundary.

i. Rate of Heavy-Load Incident (*RoHLI*)

The indicator *RoHLI* is expressed as:

$$RoHLI = \sum_{t \in T} n\left(\Omega_{\text{Line},t}^{\text{HL}}\right) / \left[n\left(\Omega_{\text{Line}}\right) \cdot n\left(T\right) \right] \tag{7}$$

$$Line_{ij} \in \Omega_{\text{Line},t}^{\text{HL}},\ \ if\ \ \left|P_{ij}\right| \geq 0.7 P_{ij}^{\max} \tag{8}$$

This indicator reflects the frequency of heavy-load incident occurring during time period *T*. The larger the indicator is, the closer the system is to the transmission limit.

ii. Rate of Voltage Off-limit Incident (*RoVOI*)

The indicator *RoVOI* is expressed as:

$$RoVOI = \sum_{t \in T} n\left(\Omega_{\text{Node},t}^{\text{VL}}\right) / \left[n\left(\Omega_{\text{Node}}\right) \cdot n\left(T\right) \right] \tag{9}$$

where $\Omega_{\text{Node},t}^{\text{VL}}$ is the set of nodes with voltage beyond the limit at the time point of *t*, which is:

$$Node_{ij} \in \Omega_{\text{Node},t}^{\text{VL}}, if\ \ U_i \geq 1.05 p.u.\ or U_i \leq 0.95 p.u. \tag{10}$$

This indicator reflects the frequency of the event that the voltage exceeds the limit during time period *T*. The larger the indicator is, the closer the system is to the voltage limit.

iii. Mean value of power that exceed the limit (*MPE*)

The indicator *MPE* is expressed as:

$$MPE = \sum_{t\in T}\sum_{Line_{ij}\in\Omega^{\mathrm{HL}}_{\mathrm{Line},t}} \left(\left|P_{ij,t}\right| - 0.7P_{ij}^{\max}\right) / \sum_{t\in T} n\left(\Omega^{\mathrm{HL}}_{\mathrm{Line},t}\right) \tag{11}$$

This indicator represents the range of lines that are beyond the power flow boundary. The larger the indicator is, the larger states fluctuation owing to renewable energy is.

iv. Extreme deviation value of Voltage (*EVV*)

The indicator EVV is expressed as:

$$EVV = \max\left\{\max(\boldsymbol{V}) - 1.05, 0.95 - \min(\boldsymbol{V})\right\} \tag{12}$$

where $\boldsymbol{V}$ is the voltage vectors of the node. *EVV* is the maximum voltage deviation in the whole time period. The larger the indicator is, the larger states fluctuation owing to renewable energy is.

3.2. Evaluation methods

To evaluate the coupling characteristics accurately, detailed simulation of the real production process is needed. Considering the participation of flexibility resources to mitigate excessive fluctuation in practice, an economic dispatching model considering mitigation effect is adopted to simulate the practical operation of the grid. Meanwhile, due to the advantages of DC transmission when dealing with the renewable energy, DC transmission is taken into consideration in the model. At the same time, in order to evaluate the voltage distribution of the system, the method in [14] is used to calculate the voltage of each node based on the DC power flow result.

1) The economic dispatch model considering system's mitigation effect on volatility

a) Objective function

In addition to minimizing total cost of power generation, the mitigation effect of is also considered in the objective:

$$obj \quad \min F = f(OC) + \lambda \cdot RoHLI \tag{13}$$

$$OC = \sum_{t\in T}\sum_{i\in\Omega_{\mathrm{G}}} c_i P_{\mathrm{G}i,t} \tag{14}$$

$$f(OC) = \frac{OC}{C^{REF}} \tag{15}$$

where *OC* represents total cost of power generation, $PG_{i,t}$ indicates the generated power for node *i* and at time *t*, c_i is the unit generation cost. Function *f*( ) is to standardize the total cost of power generation, and C^{REF} is the reference value of total cost of power generation. The larger the value of λ is, the more important of the mitigation requirement is in the system operation.

b) Constraints

Restricts to abandon renewable energy:

$$0 \le P_{\mathrm{RE},i,t} \le P^{\max}_{\mathrm{RE},i,t} \quad i \in \Omega_{\mathrm{RE}} \tag{16}$$

Restricts for the capacity of DC line:

$$-P_{ij}^{\mathrm{DCmax}} \le P_{ij}^{\mathrm{DC}} \le P_{ij}^{\mathrm{DCmax}} \quad Line_{ij} \in \Omega^{\mathrm{DC}}_{\mathrm{Line}} \tag{17}$$

Restricts for the capacity of AC line:

$$-P_{ij}^{\mathrm{ACmax}} \le P_{ij}^{\mathrm{AC}} \le P_{ij}^{\mathrm{ACmax}} \quad Line_{ij} \in \Omega^{\mathrm{AC}}_{\mathrm{Line}} \tag{18}$$

The power balance of each node:

$$P_{\mathrm{G}i,t}+P_{\mathrm{RE}i,t}-P_{\mathrm{L}i,t}=\sum_{Line_{ij}\in\Omega_{\mathrm{Line}}^{\mathrm{from},i}}P_{ij,t}^{\mathrm{AC}}+\sum_{Line_{ij}\in\Omega_{\mathrm{Line}}^{\mathrm{from},i}}P_{ij,t}^{\mathrm{DC}}-\sum_{Line_{ij}\in\Omega_{\mathrm{Line}}^{\mathrm{to},i}}P_{ij,t}^{\mathrm{AC}}-\sum_{Line_{ij}\in\Omega_{\mathrm{Line}}^{\mathrm{to},i}}P_{ij,t}^{\mathrm{DC}} \tag{19}$$

The other constraints consist of thermal generation output limit and ramp capacity limit, voltage phase limit and DC power flow.

The calculation of *RoHLI*:

$$n\left(\Omega_{\mathrm{Line},t}^{\mathrm{HL}}\right)=\sum_{Line_{ij}\in\Omega_{\mathrm{Line}}^{\mathrm{AC}}}I_{ij,t}^{\mathrm{HL}} \tag{20}$$

$$I_{ij,t}^{\mathrm{HL}}=\begin{cases}1 & \left|P_{ij,t}^{\mathrm{AC}}\right|\geq 0.7P_{ij}^{\mathrm{AC\,max}}\\ 0 & else\end{cases} \tag{21}$$

c) Linearization

While (21) is not a linear function, auxiliary variables $u_{ij,t}^{\mathrm{I}}$, $u_{ij,t}^{\mathrm{II}}$, $u_{ij,t}^{\mathrm{III}}$ can be introduced for linearization.

$$P_{ij,t}^{\mathrm{AC}}=u_{ij,t}^{\mathrm{I}}P_{ij,t}^{\mathrm{AC,I}}+u_{ij,t}^{\mathrm{II}}P_{ij,t}^{\mathrm{AC,II}}+u_{ij,t}^{\mathrm{III}}P_{ij,t}^{\mathrm{AC,III}} \tag{22}$$

$$-u_{ij,t}^{\mathrm{I}}P_{ij}^{\mathrm{AC,max}}\leq P_{ij,t}^{\mathrm{AC,I}}<-0.7u_{ij,t}^{\mathrm{I}}P_{ij}^{\mathrm{AC,max}} \tag{23}$$

$$-0.7u_{ij,t}^{\mathrm{II}}P_{ij}^{\mathrm{AC,max}}\leq P_{ij,t}^{\mathrm{AC,II}}\leq 0.7u_{ij,t}^{\mathrm{II}}P_{ij}^{\mathrm{AC,max}} \tag{24}$$

$$0.7u_{ij,t}^{\mathrm{III}}P_{ij}^{\mathrm{AC,max}}<P_{ij,t}^{\mathrm{AC,II}}\leq u_{ij,t}^{\mathrm{III}}P_{ij}^{\mathrm{AC,max}} \tag{25}$$

$$u_{ij,t}^{\mathrm{I}}+u_{ij,t}^{\mathrm{II}}+u_{ij,t}^{\mathrm{III}}=1 \tag{26}$$

$$u_{ij,t}^{\mathrm{I}},u_{ij,t}^{\mathrm{II}},u_{ij,t}^{\mathrm{III}}=0,1 \tag{27}$$

$$I_{ij,t}^{\mathrm{HL}}=u_{ij,t}^{\mathrm{I}}+u_{ij,t}^{\mathrm{III}} \tag{28}$$

From (22) to (28), the model can be transformed into a mixed integer linear programming(MILP) problem, and can be solved by commercial software(such as CPLEX).

2）Calculation of voltage distribution

We use the method proposed in [14] to calculate voltage distribution based on the result of DC power flow.

4. Hybrid AC/DC Grid Planning Considering Coupling Reducing

A bi-level stochastic programming model adopting DC lines is established in this study for grid planning. Meanwhile, as the problem related to voltage can be solved by local reactive power compensation devices, our programming model mainly focuses on the problem of heavy-load lines caused by renewable energy fluctuations.

The planning process is shown as Fig.1. The upper level is to make investment decision, and then transmit construction plan **X** to the lower level. The lower level contains production simulation module with operation state evaluation. The simulated operation status **S** is evaluated and finally, the lower level returns operation cost OC and the risk index **E** (*RoHLI* is adopted here) to the upper level.

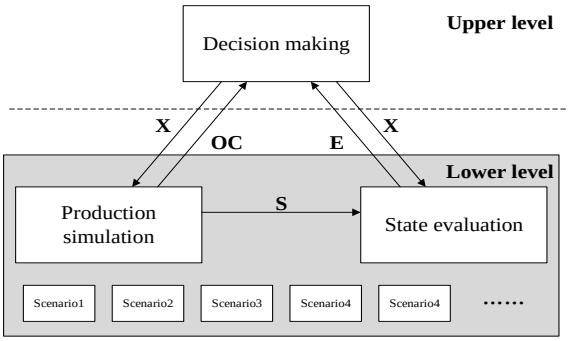

Fig. 1. Planning process considering reducing coupling.

Upper level:

$$\min \ IC + OC \tag{29}$$

$$IC = c_{ij}^{\mathrm{AC}} z_{ij}^{\mathrm{AC}} + c_{ij}^{\mathrm{DC}} z_{ij}^{\mathrm{DC}} \tag{30}$$

$$s.t. \ \ RoHLI \le RoHLI_0 \tag{31}$$

where IC is the investment cost of the system. c_{ij}^{AC} and c_{ij}^{DC} are the construction cost of AC and DC lines, separately; z_{ij}^{AC} and z_{ij}^{DC} are 0-1 variables with 1 representing constructing AC/DC lines. The constraint is that $RoHLI$ is smaller than threshold.

Lower level:

OC and $RoHLI$ are calculated. It is worth noting that as the output of renewable energy is variable, multi-scenario technique is used to make simulation result closer to the practical situation. In this paper, we adopt Affinity Propagation Clustering Algorithm to generate multiple renewable energy output scenarios and simulate with each scenario [15]. Then the integrated result is obtained by:

$$OC = \sum_{k \in \Omega_S} p_k \cdot OC_k \tag{32}$$

$$RoHOI = \sum_{k \in \Omega_S} p_k \cdot RoHOI_k \tag{33}$$

where p_k indicates the probability of the kth scenario, Ω_S is the set of scenarios, OC_k and $RoHOI_k$ are the operation cost and the risk indicator, respectively.

As the decision making and production simulation process contains a huge amount of integer variables, causing problems of large-scale optimization and huge time-consumption, heuristic method is adopted in this problem.

Detailed methods are shown as follows: the system makes investment decisions on a round-by-round basis. In each round of decision making, candidate lines are selected one by one to add to the system. Denote the line added as Line_{ij} with investment cost c_{ij}. Calculate beneficial index $I_{ij}=F_{ij}/c_{ij}$ for all candidate lines and the line with the largest I is selected as the optimal result in this round. Calculation rounds are repeated until $RoHLI$ satisfies the threshold which is set before.

5. Case Study

Fig. 2 shows a simplified grid of a province in northwestern China, which can represent typical characteristics of grid with large-scale renewable energy integration in China. There are 47 nodes, 3 of which transmitting energy to external system, which is marked as OUT in Fig. 2, and 104 lines in the system. The system is summarized in Table 1. The proportion of wind power generation capacity is about 50% and part of the wind power needs to be sent out through the local grid.

Table 1. Generation and demand in GS system

Wind power generation capacity/MW	12300
Conventional generator capacity/MW	12800
Local load/MW	11011
Power transmitted to the external system/MW	6800

5.1. Analysis in a typical day

The operation status and coupling characteristics in a typical day are analyzed and shown in Fig.2. The λ is taken as 1 in the analysis. Different colors indicate the proportion of time that the power flow or voltage exceeds the limit.

As shown in Fig. 2, the problem that power flow and voltage exceed the limit is serious. The lines whose power flow is close to the limit are mostly lines in local grid connected with renewable energy and conventional generators. This mainly due to the large amount of power provided to the local grid when the wind is strong, and the need for conventional generators in the local grid to increase their output to support load when the wind is weak. The coupling indicators of the system are shown in TABLE 2.

It can be seen that the nodes with the two functions account for about 74% of the whole system. In average, the lines whose power flow exceed the limit at each time is about 5% and the over-limit power flow of lines whose power flow exceed the limit is about 20% of the rated capacity. The nodes whose voltage exceed the limit account for about 9%, and the minimum voltage is below the limit value of 0.065. Therefore, the coupling of the system is significant.

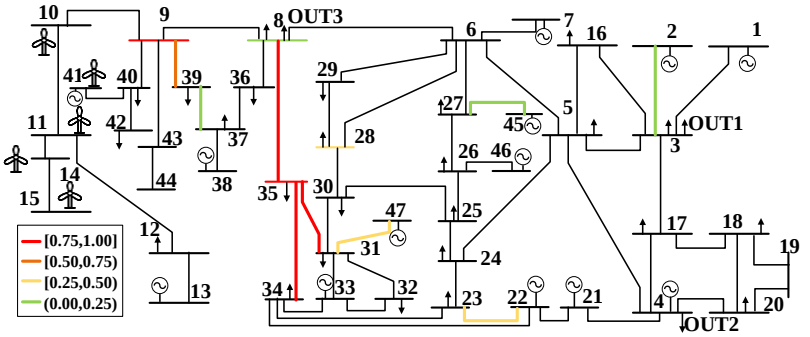

Fig. 2. The operation status in a typical day.

Table 2. Evaluation Result of GS System

indicator	***RoC***	***RoHLI***	***RoVOI***	***MPE***	***EVV***
value	0.7447	5.4%	9.3%	20.2%	0.065

5.2. Planning results

Set the threshold of *RoHLI* to 1.5%. AC candidate lines are set following the principle that new lines are available in all existing right-of-ways but the number of lines on each right-of-way cannot exceeds 3. For DC candidate lines, all DC lines can be built in the place where the AC line can be built. At the same time, there are 5 more candidate lines, which are DC6-45, DC6-46, DC5-46, DC5-47, DC8-47. These lines provide direct connection between local generators and renewable energy transmission lines to reduce the impact of uncertainty with renewable energy on the local grid.

The cost of DC transmission consists of two parts, the line cost and the cost of the converter station. Assume that the DC voltage level is ±300kV with transmission capacity being 1000MW. The cost parameter is in [16]. The AC line is assumed to be 330kV, and the cost parameter of which is in [17].

The results of planning with hybrid AC/DC transmission and only AC transmission are shown in Table 3, in which the order of the planning scheme from the top to bottom is the order in which the lines are added to the system each round.

Table 3. Planning result comparison

Parameter	Hybrid AC/DC	AC only
Planning result	AC31-47 DC8-47 DC8-36	AC31-47 AC9-39 AC37-39 AC27-45 AC22-23
Operation cost(M$/y)	2379	2703
Investment cost(M$) (equivalent annual value)	167	120
Total cost(M$)	2546	2823

AC lines are adopted in the planning results bringing economic advantages. At the same time, due to the flexibility of DC transmission, the DC lines are installed to cope with the uncertainty. It is worth noting that the line DC8-47 connects the generator directly to the renewable energy transmission right-of-way. It can be inferred that this strategy can effectively improve the performance of the system when dealing with fluctuation with renewable energy. Compare the results of hybrid AC/DC with only AC transmission, it can be seen that to achieve same threshold, planning only with AC transmission requires more lines, and the operation cost is greater. Plans with DC transmission can significantly reduce the operation cost while helping to stabilize system states. Besides, the hybrid AC/DC planning scheme has lower cost, which rationalize the installation of DC transmission systems.

6. Conclusion

In this paper, to deal with the problem of coupling between renewable energy and the system state in the grid with high proportion of renewable energy, the evaluation indicators and methods are proposed from the perspective of network structure and operation states. The evaluation index is included in the AC/DC transmission expansion planning. The case study shows:

(1) The coupling of the grid with the integration of large-scale renewable energy are obvious and the proposed indicators can reflect the effect of coupling;

(2) The structure of the power grid with hybrid AC/DC transmission significantly affects the coupling of the system. The reduction of coupling in the hybrid AC/DC transmission system is greater than that in the AC system.

Conflict of Interest

No potential conflict of interest was reported by the authors.

Author Contributions

Zongxiang Lu developed the idea for the study. Hao Li designed and performed the research, analyzed data, and wrote the paper. Ying Qiao revised the manuscript.

Acknowledgements

Project Supported by State Grid as ‘Research on Temporal and Spatial Equilibrium Method of Power System Flexibility Based on Hybrid Probability Optimization’.

References

[1] Nordic Wind Energy Center (2018). [Online]. Available: https://www.nordisktvindenergicenter.eu. Accessed 10 Nov 2018

[2] China Energy Storage Alliance (2018) Renewable Integration Update: Northwest China. [Online]. Available: http://en.cnesa.org/latest-news/2016/8/19/renewable-integration-update-northwest-china. Accessed 10 Nov 2018

[3] Beijixing Electic (2018) Wind turbine disconnection accidents. [Online]. Available:

http://news.bjx.com.cn/html/20111202/327304.shtml. Accessed 10 Nov 2018

[4] George SO, George HB, and Nguyen SV. Risk Quantification Associated With Wind Energy Intermittency in California. *IEEE Transactions on Power Systems*, 2011, 26, (4), pp. 1937-1944.

[5] Ueckerdt F, Brecha R, and Luderer G. Analyzing major challenges of wind and solar variability in power systems. *Renewable Energy*, 2015; 81: 1-10.

[6] Yuan B, Zhou M, and Zong J. An overview on peak regulation of wind power integrated power systems. In: *Proc. of 2011 4th International Conference on Electric Utility Deregulation and Restructuring and Power Technologies (DRPT)*, 2011; 145-150: IEEE.

[7] Lotfjou A, Fu Y, and Shahidehpour M. Hybrid AC/DC transmission expansion planning. *IEEE Transactions on Power Delivery*, 2012; 27(3):1620-1628.

[8] Dominguez AH, Macedo LH, Escobar AH, and Romero R. Multistage security-constrained HVAC/HVDC transmission expansion planning with a reduced search space. *IEEE Transactions on Power Systems*, 2017; 32(6): 4805-4817.

[9] Dominguez AH, Escobar AH, and Gallego RA. An MILP model for the static transmission expansion planning problem including HVAC/HVDC links, security constraints and power losses with a reduced search space. *Electr Pow Syst Res*, 2017; 143: 611-623.

[10] Dominguez AH, Zuluaga AHE, Macedo LH, and Romero R. Transmission network expansion planning considering HVAC/HVDC lines and technical losses. Proc Ieee-Pes, 2016

[11] Doagou-Mojarrad H, Rastegar H, and Gharehpetian GB. Probabilistic multi-objective HVDC/AC transmission expansion planning considering distant wind/solar farms. *Iet Sci Meas Technol*, 2016; 10(2): 140-149.

[12] Wu Z, Liu P, Gu W, Huang H, and Han J. A bi-level planning approach for hybrid AC-DC distribution system considering N-1 security criterion. *Applied Energy*, 2018; 230: 417-428.

[13] Acha E, Fuerte, Esquivel CR, and AmbrizPerez H. Topological generation and load distribution factors for supplement charge allocation in transmission open access – Discussion. *IEEE Transactions on Power Systems*, 1997;12(3): 1185-1193.

[14] Liu D, Cheng H, Fang S, et al. DC power flow celculation method considering voltage and reactive power. *Power System Technology*, 2017; 41(8): 58-62. [in Chinese]

[15] Frey BJ, and Dueck D. Clustering by passing messages between data points. *Science*, 2007;315, (5814): 972-976.

[16] Feng W, Tuan LA, Tjernberg LB, Mannikoff A, and Bergman A. A New approach for benefit evaluation of multiterminal VSC-HVDC using a proposed mixed AC/DC optimal power flow. *IEEE Transactions on Power Delivery*, 2014; 29(1): 432-443

[17] Tim M, Trevor C, and Dan W. Capital costs for transmission and substations: Recommendations for WECC transmission expansion planning, Oct. 2014. [Online]. Avaliable: https://www.wecc.biz/Reliability/2014_TEPPC_Transmission_CapCost_Report_B+V.pdf